Environ. Sci. Technol. **2001**, *35,* 1688−1695

A Distributed Reactivity Model for Sorption by Soils and Sediments. 14. Characterization and Modeling of Phenanthrene Desorption Rates

MARTIN D. JOHNSON,
T. MICHAEL KEINATH II, AND
WALTER J. WEBER, JR.*

Environmental and Water Resources Engineering, Department of Civil and Environmental Engineering, The University of Michigan, Ann Arbor, Michigan 48109-2125

Rates and extents of phenanthrene desorption were studied for more than 250 days as functions of sorbent type, initial loading level, and aging. Apparent first-order desorption rate constants for the slowly desorbing fraction were found to (i) range from 0.00086 to 0.148 days^{-1} for geosorbents that contain geologically mature kerogen and less rigid humic-type soil organic matter, respectively, (ii) decrease by as much as an order of magnitude with decreasing initial sorbed solid-phase phenanthrene concentration, (iii) decrease by a factor of 2 with increasing aging time for a humic topsoil but remain unaffected by aging time beyond 3 months for a shale, and (iv) be 1−2 orders of magnitude lower than rate constants for the rapidly desorbing phenanthrene fractions for any given contaminated sample. Six models were used to fit the desorption rate data. Biphasic diffusion and biphasic first-order models with three fitting parameters possess broad utility and are potentially useful in a variety of environmental applications. Disadvantages of a five-parameter triphasic first-order desorption model, a two-parameter gamma-function model, and a one- or two-parameter pore diffusion model are also discussed.

Introduction

Rates of desorption associated with the release of hydrophobic organic contaminants (HOCs) from soils and sediments into interstitial water are at least biphasic, with an initial rapid desorption phase that occurs over a few hours or days followed by an extremely slow desorption that can take months or years to reach an endpoint (*1*−*5*). The latter phase, which may result in a significant fraction being effectively sequestered (*2*−*10*), is frequently rate-limiting for biodegradation, bioremediation, and subsurface transport (*5, 11*−*16*). Mechanisms proposed as potentially responsible for the commonly observed slow desorption of HOCs from soils and sediments include intraorganic matter diffusion (*2, 3, 17, 18*) and hindered pore diffusion (*5, 19*−*25*). Diffusion through soil organic matter is analogous to diffusion in polymers; i.e., diffusing molecules must penetrate and migrate through a polymeric matrix (*26*−*28*). Pore diffusion can be either sterically hindered or retarded by sorption to organic phases associated with pore walls. Desorption from high energy sites may also be an important rate limiting step. In condensed polymeric organic matter, HOCs may sorb strongly in molecular size voids or "holes" (*28, 29*), while during pore diffusion they are subject to high energy sorption in molecular size pores (*5, 24, 30, 31*). Thus, slow desorption has been modeled both as a diffusion and as a first-order rate process. Several different rate models have been used to describe desorption of HOCs from natural sorbents; six of these are compared in this study.

Despite findings indicating that effective time scales for slow desorption processes are on the order of months to years, most desorption experiments have been measured only for short time periods; e.g., over durations of 0.1−8 days (*6, 10, 22, 25, 32*−*34*) and/or 1−5 weeks (*1, 4, 7, 21, 23, 24, 30, 31, 35*−*38*). A few studies have measured desorption rates and extents over longer periods, 1−3 months (*3, 8, 39*), and/or 0.5−1 year (*2, 40*). Several of the shorter studies have led to conclusions regarding mechanisms that might not have been advanced or supported had the observation time scales been extended. The desorption experiments discussed in this study were measured over periods of more than 250 days.

When present in concentrations above about 0.1%, natural soil/sediment organic matter (SOM) dominates the HOC desorption process (*1*−*3, 9, 17, 18, 21, 34, 36, 41*). Furthermore, the type of natural organic matter involved affects apparent sorption desorption hysteresis. Natural sorbents that contain physically condensed, chemically reduced, geologically mature kerogen-like organic material are characterized by significant desorption hysteresis, while sorbents with geologically immature, more labile, humic acid types of organic matter exhibit little or no desorption hysteresis (*42, 43*). This study compares phenanthrene desorption from a topsoil having humic-like SOM, a shale having kerogen-like SOM, and a sandy soil containing shale particles.

Desorption rates and resistant fractions are a function of initial solid-phase HOC loading (*5, 7, 22, 24, 30, 34, 38, 44, 45*). In general, sorption and desorption rate constants increase and resistant fractions decrease with increasing sorbate concentration levels. This study investigates desorption as a function of initial solid-phase phenanthrene loading levels.

Rates and extents of HOC desorption from soils or sediments decrease with increasing contact time, a phenomenon commonly referred to as the aging effect. For field contaminated samples that have been "aged" for years or decades, desorption-resistant HOC fractions can be 15−20 times higher than for laboratory-spiked samples (*4, 5*), although comparisons of field-contaminated samples to laboratory-spiked samples can be biased by the desorption or degradation of rapidly released HOC fractions prior to field collection. Aging effects have also been reported for strictly laboratory-spiked samples, with desorption resistant fractions increasing by factors of 2−10 as a function of aging time (*1, 3, 25, 31*−*35, 38*). However, in each of these studies the short aging times were only 0.1−5 days; i.e., not long enough to establish an initial sorption equilibrium, which actually requires weeks or months of incubation for most HOC/geosorbent systems (*3, 28, 29, 44, 46*). A more practical concern from a remediation standpoint is the effect of aging beyond initial HOC/sorbent equilibrium. In fact, some previous studies have shown that aging beyond 3 weeks to several months has negligible additional effect on desorption-resistant fractions or release rates (*1, 6, 22*−*24, 30, 31, 34*). Therefore, in contrast to most literature reports on aging

* Corresponding author phone: (734)763-2274; fax: (734)763-2275; e-mail: wjwjr@engin.umich.edu.

10.1021/es001391k CCC: $20.00
Published on Web 03/09/2001

effects, this study considers the aging effect in systems where both "short" and "long" incubation times (3 months and 1 year, respectively) are sufficiently long for the HOC/sorbent systems to obtain apparent sorption equilibrium prior to initiation of desorption.

Materials and Methods

Solute. Phenanthrene obtained from Aldrich Chemical Co. in spectrophotometric-grade was utilized as a probe HOC for these desorption experiments. Phenanthrene solubility at 25 °C is about 1200 μg/L (*47*) and its log K_{ow} is 4.568 (*48*).

Geosorbents. The natural sorbents were chosen on the basis of the functional properties of their associated SOM. Chelsea soil (particle size <2000 μm), a geologically young topsoil collected near Chelsea, MI, contains SOM (5.62 wt % organic carbon) having extractable humic and fulvic acid organic matter characteristics. Lachine shale (63−180 μm), collected near Alpena, MI, is a geologically older sediment containing SOM (8.27 wt % organic carbon) comprised primarily of type II kerogen. Kerogen, as opposed to the organic matter of Chelsea soil, is relatively nonextractable, chemically reduced, and physically condensed (*49, 50*). Shale is a significant sorption compartment of aquifer materials that contain glacial outwash or till, such as Wagner soil. Wagner soil (450−500 μm) is a sandy soil with 0.5% (by weight) organic carbon, mostly in the form of intermixed shale particles. Previous publications in this Distributed Reactivity Model (DRM) series of papers have characterized the properties and sorption behaviors of the Chelsea soil (*51*−*55*), Lachine shale (*43, 44*), and Wagner soil (*56, 57*).

Sorbent Loading for Desorption Experiments. The sorbents were exposed to the probe HOC in 1-L glass bottles filled with buffer solution and a predetermined mass of solid phenanthrene crystals. The buffer solutions contained 0.005-M $CaCl_2$ as a mineral constituent, 100 mg/L of NaN_3 to inhibit biological activity, and 0.005 g/L of $NaHCO_3$ to buffer at pH 7.0. The spiked reactors were mixed end-over-end on a tumbler at 12 rpm for the first month of phenanthrene contact to ensure CMBR (completely mixed batch reactor) conditions, after which the bottles were stored at 25 °C and manually agitated weekly for the remainder of the aging period, either 3 months or 1 year. Low, mid, and high loading levels were accomplished by adding appropriate amounts of phenanthrene crystals to the CMBR, predetermined through 3-month sorption isotherms, so that corresponding final aqueous phase equilibrium concentrations were approximately 20, 300, and 800 μg/L, respectively. Additional details regarding the spiking experiments are given in an earlier paper (*58*). To ensure accurate solid-phase phenanthrene concentrations and establish a baseline for subsequent desorption experiments, a mass balance was determined at the end of the aging stage by analysis of aqueous-phase and solid-phase phenanthrene concentrations, the latter by either 24-h methanol Soxhlet extractions or 250 °C subcritical water extraction (*59*). The subcritical water extractions proved more effective than the methanol Soxhlet extractions. Overall mass balances for all contaminated geosorbents were between 95 and 105%, indicating that experimental losses and microbial degradation were negligible.

Phenanthrene Desorption Rates. Rate experiments at 25 °C were conducted as described in the earlier paper referenced above (*58*), using Tenax polymeric resin to maintain an infinite-dilution condition. The desorption CMBRs were flame-sealed glass ampules containing the Tenax, phenanthrene contaminated soil, and aqueous buffer that were mixed continuously on a shaker table. Several reactors having identical contents were run in parallel for each contaminated sample. At selected times throughout the experiment a single ampule from the set was opened, the Tenax, aqueous, and geosorbent phases separated, and the total mass of phenanthrene sorbed to the Tenax phase analyzed. In this manner, each CMBR was used to generate a single point on a desorption profile.

Because of the density differences between soil and Tenax, separation of these materials was accomplished by centrifugation at 1000 G for 1 h. Residual soil was rinsed from the separated Tenax with centrifuged solution. Corrections were made for the quantified amount (0.1−1%) of Tenax that "sank" to the bottom of each ampule. Samples of the aqueous phase were taken for each quenched CMBR to verify that the solution phase phenanthrene concentration was negligible (<1 μg/L). Phenanthrene was extracted from the Tenax beads using hexane, and the phenanthrene concentration in the hexane was determined by HPLC with UV detection.

Mass balances of phenanthrene were within 90−110% of the total added for all reported data, indicating that unaccounted losses and microbial activity were negligible. This desorption rate technique has advantages over common experimental methods. Desorption rate curves are not additive because a separate CMBR generates each point, so errors are not propagated through addition of each sequential desorbed fraction, and mass balances can be closed for each point on the desorption curve. Additionally, flame-sealed glass ampules minimize phenanthrene loss, so desorption steps can be performed for several months with no significant losses.

Phenanthrene Measurement. All phenanthrene concentrations were analyzed by reverse-phase HPLC (Hewlett-Packard Model 1090, ODS, 5 micron, 2.1 × 250 mm column) with UV detection for concentrations between 10 and 1000 μg/L and fluorescence detection for concentrations between 0.1 and 10 μg/L.

Modeling. Six models variously used to describe desorption phenomena were evaluated for description of the rate data measured in this work. Brief descriptions of these models follow.

The first two models tested are similar in form, each being a three-parameter, two-compartment model. One of these uses first-order equations to describe desorption rates for both the slowly desorbing fraction, ϕ_s, and the rapidly desorbing fraction, ϕ_r (= 1 − ϕ_s) (*35*); i.e.,

$$\frac{q(t)}{q_o} = \phi_s \exp(-k_s t) + (1 - \phi_s)\exp(-k_r t) \qquad (1)$$

where $q(t)$ is the solid-phase sorbate concentration at a given time, q_o is the initial solid-phase sorbate concentration, and k_s and k_r are apparent first-order rate constants for the slowly and rapidly desorbing fractions, respectively. This empirical model is similar in form to that proposed by Karickhoff (*36*), except that in his model instantaneous equilibrium was assumed for the rapidly desorbing compartment. The second three-parameter, two-compartment model assumes biphasic polymer diffusion processes. The model was originally developed to analyze rates of desorption of solutes from poly(vinyl chloride) polymer powders of nonuniform particle size (*61, 62*) but has also been used to describe HOC desorption from sediments (*2*), i.e.,

$$\frac{q(t)}{q_o} = \frac{6}{\pi^2}\sum_{n=1}^{\infty}\frac{1}{n^2}\left[\phi_r \exp\left(\frac{-4n^2\pi^2 D_r t}{a_r^2}\right) + (1 - \phi_r)\exp\left(\frac{-4n^2\pi^2 D_s t}{a_s^2}\right)\right] \qquad (2)$$

where ϕ_r is again the rapidly desorbing fraction, D_r and D_s

are diffusion coefficients for rapidly and slowly diffusing fractions, and a_r and a_s are the corresponding equivalent sphere diameters. The model is solved for ϕ_r, (D_r/a_r^2), and (D_s/a_s^2).

The third model tested is a five-parameter, three-compartment model that assumes a triphasic desorption process in which the slow fraction is divided into two compartments, slowly desorbing and very slowly desorbing ($\phi_{vs} = 1 - \phi_r - \phi_s$) (*7, 8, 21, 39*); it has the form

$$\frac{q(t)}{q_o} = \phi_r \exp(-k_r t) + \phi_s \exp(-k_s t) + (1 - \phi_r - \phi_s)\exp(-k_{vs} t) \quad (3)$$

The fourth model evaluated is a two-parameter model based on the statistical gamma function. This "gamma" model assumes that desorption from heterogeneous sites occurs over a continuum of energies and rates (*6, 46, 60*). This model has the form

$$\frac{q(t)}{q_o} = 1 - \left(\frac{\beta}{\beta + t}\right)^{\alpha} \quad (4)$$

where the probability that a molecule is desorbing from a compartment with desorption rate "k" is described by the gamma density function $f(k)$ with a normalization factor Γ; i.e.,

$$f(k) = \frac{\beta^{\alpha} k^{\alpha-1} \exp(-\beta k)}{\Gamma(\alpha)}, \; \Gamma(\alpha) = \int_0^{\infty} x^{\alpha-1} \exp(-x) dx \quad (5)$$

The mean and standard deviation of the desorption rates are described by

$$E(k) = \frac{\alpha}{\beta} \text{ and } \sigma(k) = \frac{\alpha^{1/2}}{\beta} \quad (6)$$

An advantage of this model is that it theoretically describes a continuous distribution of sorptive compartments with only two parameters, α and β.

A one-parameter spherical pore-diffusion model (*20, 23–25*) was also used to describe the experimental rate data. The Crank solution to the spherical diffusion model is given by

$$\frac{q(t)}{q_o} = \frac{6}{\pi^2} \sum_{n=1}^{\infty} \frac{1}{n^2} \exp\left(\frac{-n^2 \pi^2 D_{app} t}{r^2}\right) \quad (7)$$

where D_{app} is the apparent diffusion coefficient, r is the sphere equivalent radius, and the model is solved for (D_{app}/r^2) (*63*). Advantages of this model are that it has only one fitting parameter, (D_{app}/r^2), and it can theoretically estimate desorption rates a priori based on sorbate and sorbent physical characteristics (*25*).

Last, because the simple spherical pore-diffusion model often does not fit entire desorption rate profiles, a sixth model assuming that a fraction of sorbed contaminant, X_1, attains instantaneous equilibrium (*22–24, 30, 31*) was also tested. The analytical solution to this model is

$$\frac{q(t)}{q_o} = \frac{(1 - X_1)6}{\pi^2} \sum_{n=1}^{\infty} \frac{1}{n^2} \exp\left(\frac{-n^2 \pi^2 D_{s,app} t}{r^2}\right) \quad (8)$$

where $D_{s,app}$ is an apparent diffusion coefficient for the slowly desorbing fraction. The model is solved for X_1 and $(D_{s,app}/r^2)$.

Software. The first-order models were fit to desorption rate data by the Levenberg–Marquardt nonlinear regression technique with SAS software (SAS Institute, Inc., Cary, NC). The infinite series models were fit using a Fortran program that incorporated the Levenberg–Marquardt nonlinear regression technique and included the first two thousand terms in the infinite series. This many terms are required to bring $q(t)/q_o$ within 0.1% of unity at zero time.

TABLE 1. Phenanthrene Desorption Rate Parameters for the Three-Parameter Biphasic First-Order Desorption Model with 95% Confidence Intervals

sample	ϕ_r	ϕ_s	k_r [days^{-1}]	$k_s \times 10^3$ [days^{-1}]
L1	0.144	0.856 ± 0.034	0.0450 ± 0.0213	0.896 ± 0.213
L2	0.171	0.829 ± 0.090	0.0289 ± 0.0216	0.859 ± 0.598
L3	0.314	0.686 ± 0.056	0.0894 ± 0.0408	2.41 ± 0.59
L4	0.260	0.740 ± 0.110	0.0716 ± 0.0629	2.16 ± 1.14
L5	0.367	0.633 ± 0.075	0.139 ± 0.079	2.63 ± 1.03
L6	0.360	0.640 ± 0.071	0.180 ±0.099	2.92 ± 1.03
W1	0.264	0.736 ± 0.040	0.134 ±0.055	1.38 ± 0.53
W2	0.291	0.709 ± 0.051	0.148 ± 0.069	1.82 ± 0.68
W3	0.343	0.657 ±0.045	0.332 ± 0.136	2.63 ± 0.66
C1	0.389	0.611 ± 0.049	0.320 ± 0.131	4.20 ± 1.00
C2	0.299	0.701 ± 0.051	0.592 ± 0.373	10.3 ± 2.0
C3	0.586	0.414 ± 0.102	0.625 ± 0.357	7.32 ± 4.29
C4	0.590	0.410 ± 0.172	1.29 ± 1.43	12.4 ± 12.7
C5	0.524	0.476 ± 0.150	2.30 ± 1.72	70.2 ± 46.9
C6	0.384	0.616 ± 0.107	7.30 ± 8.753	148 ± 69

Results and Discussion

Sorbent Type, Loading Level, and Aging Effects. Phenanthrene desorption rate data is shown in Figures 1–3. The model fits for each data set using the biphasic first-order rate model are included on the graphs. Corresponding desorption rate parameters with 95% confidence intervals are listed in Table 1. The legends for Figures 1–3 designate initial solid-phase phenanthrene loading levels and aging time prior to desorption for each sample. Corresponding shorthand identifications, i.e., L1–L6, W1–W3, and C1–C6, are used in all tables. We use the data and biphasic modeling results as bases for four main observations.

First, desorption rates and extents are strong functions of geosorbent type; more specifically, the type of natural organic matter that each contains. Phenanthrene desorbs from Chelsea soil at higher rates than from Wagner soil and Lachine shale. Values of k_s range from 0.0042 to 0.148 day^{-1} for Chelsea soil, 0.00138–0.00263 day^{-1} for Wagner soil, and 0.000859–0.00292 day^{-1} for Lachine shale. Corresponding values for k_r range from 0.32 to 7.3 day^{-1} for Chelsea soil, 0.134–0.332 day^{-1} for Wagner soil, and 0.029–0.180 day^{-1} for Lachine shale. Confidence intervals for these parameters are listed along with the modeling results in Table 1. Furthermore, as seen in Figures 1–3, the mass fraction of phenanthrene remaining on the sorbents after 250 days of desorption time is higher for Lachine shale (33%–68%) and Wagner soil (36%–47%) than for Chelsea soil (0%–23%). These results agree with the hypothesis that geosorbents containing less rigid, labile humic organic matter will allow faster and more complete desorption than geosorbents containing condensed kerogen. It has also been proposed that these organic matter types are analogous to rubbery and glassy polymers, respectively (*2, 17, 18, 28, 29, 51, 64*). Diffusion rates in glassy polymers are generally much slower than those in rubbery polymers (*26, 27, 61*). Additionally, condensed polymeric organic matrices may contain nanometer-size "holes" that provide complexation sites to adsorb solutes strongly (*28, 29*), thus reducing desorption rates.

Second, the rate constants and extents of desorption increase with higher initial solid-phase phenanthrene loading levels for all three sorbents. For example, Figure 1 shows that with 250 days desorption time only about 32% of the initial sorbed phenanthrene was released from the Lachine shale samples having the lowest initial loadings (L1 and L2), while

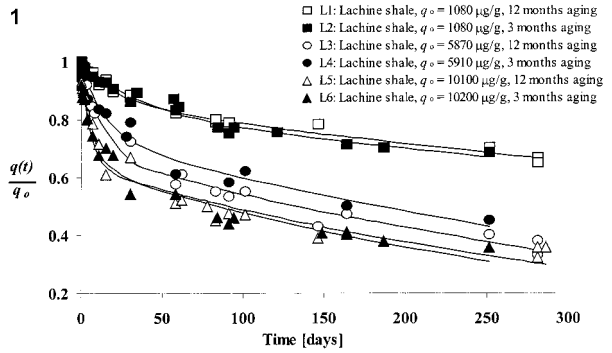

FIGURE 1. Phenanthrene desorption from Lachine shale into infinite dilution water at 25 °C as a function of initial solid-phase loading level and aging time.

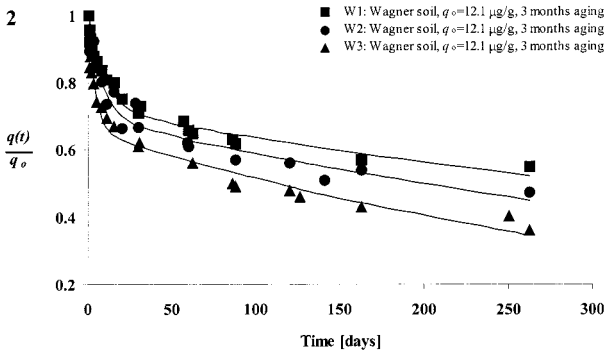

FIGURE 2. Phenanthrene desorption from Wagner soil into infinite dilution water at 25 °C as a function of initial solid-phase loading level.

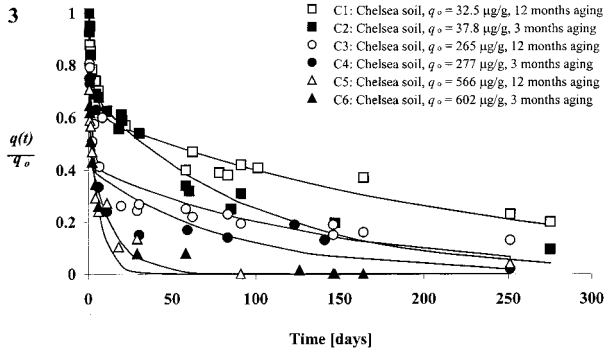

FIGURE 3. Phenanthrene desorption from Chelsea soil into infinite dilution water at 25 °C as a function of initial solid-phase loading level and aging time.

about 66% of the initial amounts of sorbed phenanthrene was released from those having the highest initial loadings (L5 and L6). Similar trends are seen in Figures 2 and 3 for the Wagner and Chelsea soils. Two explanations for this "initial" loading effect are proposed. Assuming that there is a distribution of sorption site energies associated with SOM (*56*), the higher energy sites may be occupied preferentially. Thus, at lower initial loading levels a higher percentage of sorbate molecules are sorbed to higher energy sites, which presumably involve slower desorption than do lower energy sites. Alternatively, solute diffusion through polymeric SOM matrices may be concentration dependent, in a manner analogous to that for diffusion through glassy synthetic polymers, for which higher sorbate concentrations result in higher diffusion rates (*28, 34*). Furthermore, high concentrations of sorbate can swell organic matter matrices, causing them to be more flexible and thus facilitating diffusion of solutes (*26*−*28, 51*). This is consistent with reports that phenanthrene sorption by soils and sediments approaches equilibrium significantly faster at high concentration levels than it does at low levels (*44, 45*).

Third, there may be an aging effect with Chelsea soil but not with Lachine shale. Comparing samples C1 and C2 for Chelsea soil, two samples having approximately the same values for q_o, k_s is lower for 12-month aging prior to desorption than for 3-month aging, i.e., 0.0042 ± 0.001 versus 0.010 ± 0.002 day^{-1}. On the other hand, in comparing the rate parameters for the Lachine shale samples (i.e., L1 vs L2, L3 vs L4, and L5 vs L6) there appear to be no statistically significant differences in desorption rate constants between 3-month and 12-month aged samples having similar q_o values. The lack of an aging effect for Lachine shale is also visually apparent in Figure 1.

Fourth, comparing k_s and k_r values in Table 1, the rate constant for the slowly desorbing fraction of each sample is up to 2 orders of magnitude lower than the corresponding rate constant for the rapidly desorbing fraction, the ratio of k_r/k_s values ranging from 33 to 104. These results stress the importance of accurately characterizing rates for slowly desorbing fractions in the modeling of contaminant fate and transport and the planning of associated remediation schemes. Although apparent first-order desorption rate constants for slowly desorbing fractions are about 2 orders of magnitude lower than those for rapidly desorbing fractions, many desorption studies report measured rates *only* for the rapidly desorbing fraction. In field remediation efforts, however, it is the slowly desorbing fractions that eventually control required time frames.

Model Comparisons: *Three-Parameter Biphasic First-Order Model.* Given its empirical nature, the three-parameter biphasic first-order desorption model is reasonably robust, as shown in Figures 4A−6A and previously in Figures 1−3. The model parameters summarized in Table 1 were discussed in the preceding section. Values for k_r range from 0.029 to 7.3 day^{-1} and values for k_s range from 0.00086 to 0.148 day^{-1}, depending on geosorbent type, initial phenanthrene loading level, and aging time. Literature values of k_r for HOC desorption from soils and sediments have been reported as 1−10 day^{-1} (*35*) and 0.7−12 day^{-1} (*7*), and for k_s as 0.14 day^{-1} (*6*), 0.02−0.1 day^{-1} (*35*), 0.01−0.05 day^{-1} (*7*), 0.009−0.04 day^{-1} (*1*), 0.03−1.3 day^{-1} (*36*), 0.002−0.007 day^{-1} (*3*), 0.005 day^{-1} (*2*), 0.024−0.1 day^{-1} (*39*). An advantage of this model is that its parameters are useful for distinguishing between rapidly and slowly desorbing fractions. Furthermore, model results are intuitive given the biphasic nature of the desorption data. For example, Figure 5A shows that about 35% of the sorbed phenanthrene is released from sample W3 in the first 15 days, after which the desorption rate appears to decrease by more than an order of magnitude for the next 245 days. Not surprisingly, the biphasic desorption model converges on a ϕ_s value of about 65% for sample W3, while k_r is 0.332 day^{-1} and k_s is only 0.00263 day^{-1}. For the other samples, a similar inspection of the rapid and slow phases on the desorption profiles reveals that they correspond convincingly with model results for ϕ_r and ϕ_s reported in Table 1.

Five-Parameter Triphasic First-Order Model. Table 2 lists parameters for the triphasic first-order model. Figures 4A−6A show that the triphasic model provides a good fit of desorption data in each case, which is not surprising in that it has at least two more fitting parameters than any of the other models. In support of the triphasic model, the statistical F-test at a 95% confidence level revealed that the addition of two extra parameters is statistically justified over the three-parameter biphasic desorption model for 10 of the 15 cases. Rate parameters for each of the three phases varied widely as a function of sorbent type, loading level and aging. Values for k_r, k_s, and k_{vs} ranged from 0.66 to 13.7 day^{-1}, 0.018−0.48 day^{-1}, and 0.00084−0.034 day^{-1}, respectively. The ratio k_s/

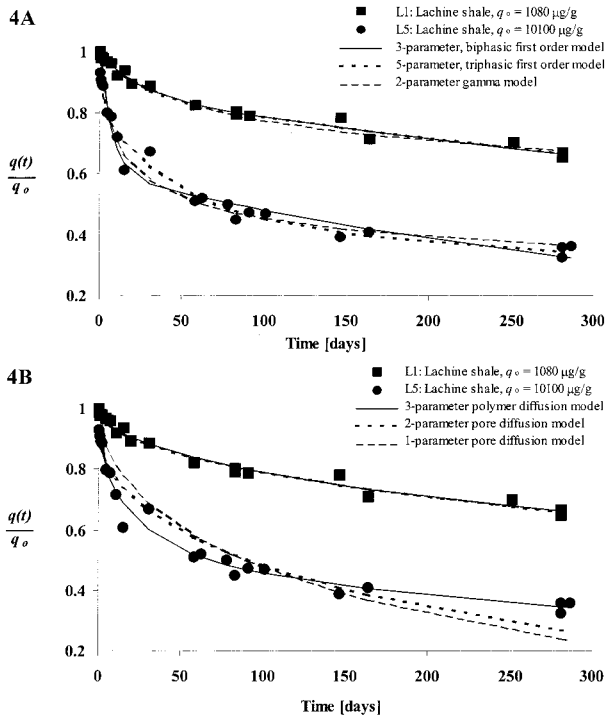

FIGURE 4. Modeling 25 °C phenanthrene desorption from Lachine shale: (A) multicompartment first-order desorption models and (B) diffusion models.

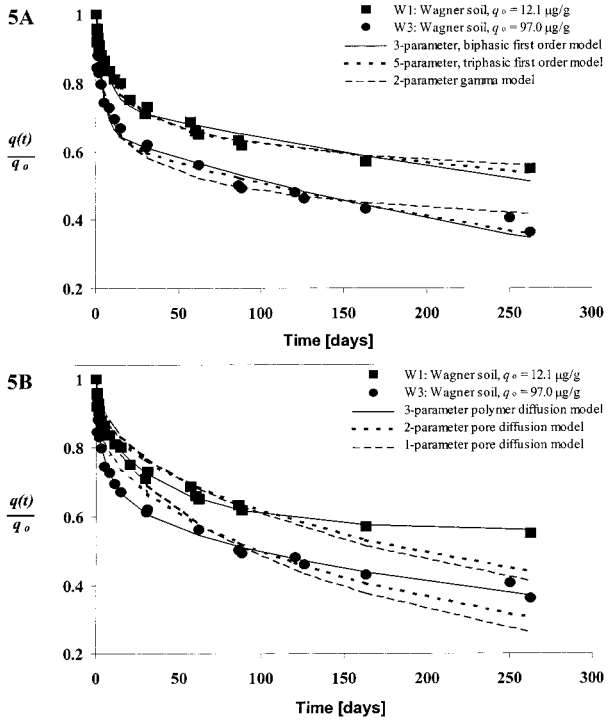

FIGURE 5. Modeling 25 °C phenanthrene desorption from Wagner soil: (A) multicompartment first-order desorption models and (B) diffusion models.

k_{vs} ranged from 6 to 58. These compare well with literature values of k_{vs} for HOC desorption from soils and sediments that are about 0.001 day^{-1} (*39*) and 0.002−0.004 day^{-1} (*8*) with k_s/k_{vs} ratios of 10−50 (*39*) and 20−170 (*8*).

It was difficult to find global minima for the sums of squared residuals because local minima were often established during the model fitting exercises. In other words, to solve the triphasic model one must know, *a priori*, how to identify the three phases in order to make appropriate initial guesses. However, the three phases were not visually obvious in the desorption curves. It has been suggested that the triphasic model divides ϕ_s from the biphasic model into a slow fraction, ϕ_s, and a very slow fraction, ϕ_{vs}, which should facilitate initial guesses (*21, 65*). However, comparison of ϕ_r in Tables 1 and 2 reveals that this is only true for samples C2 and C6. In fact, for samples W1, W2, and W3, ϕ_r (biphasic model) was divided into ϕ_r and ϕ_s (triphasic model), while ϕ_s (biphasic model) essentially became ϕ_{vs} (triphasic model). In addition, for samples L1−L3, W1−W3, and C4, k_r varied widely with no significant change in sum of squared residuals between model fit and measured data. Because convergence on a five-parameter solution was laborious and uncertain, with final fitted parameters strongly depending on initial guesses, we do not recommend the triphasic model over the biphasic desorption model.

TABLE 2. Phenanthrene Desorption Rate Parameters for the Five-Parameter Triphasic First-Order Desorption Model

sample	ϕ_r	ϕ_s	ϕ_{vs}	k_r [days^{-1}]	$k_s \times 10^3$ [days^{-1}]	$k_{vs} \times 10^3$ [days^{-1}]
L1	0.0146	0.136	0.85	5−10.4−100	34.2	0.874
L2	0.0624	0.264	0.673	5.48−12.9	75.2	1.46
L3	0.0555	0.305	0.64	9−13−100	39.4	2.06
L4	0.0919	0.277	0.631	1.19	22.8	1.36
L5	0.189	0.354	0.457	0.662	21.8	1.02
L6	0.104	0.351	0.545	5.44	60.9	1.83
W1	0.00774	0.251	0.672	2.54−10	45.0	0.839
W2	0.062	0.263	0.674	5.55−9.95	75.9	1.48
W3	0.090	0.280	0.630	10−300	126	2.16
C1	0.206	0.265	0.529	1.09	61.6	3.12
C2	0.266	0.528	0.206	0.700	17.5	2.73
C3	0.21	0.507	0.284	13.7	146	3.37
C4	0.205	0.610	0.185	35−65	163	3.33
C5	0.272	0.434	0.294	8.97	481	33.8
C6	0.345	0.492	0.163	10.4	259	18.1

TABLE 3. Phenanthrene Desorption Rate Parameters for the Two-Parameter Gamma Model

sample	α	β [days]	mean k_d [a] [days^{-1}]	σ (k_d)[b] [days^{-1}]
L1	0.145	20.7	0.00700	0.0184
L2	0.160	24.0	0.00667	0.0167
L3	0.284	10.4	0.02731	0.0512
L4	0.232	10.2	0.0228	0.0472
L5	0.221	3.05	0.0725	0.154
L6	0.205	2.08	0.0986	0.218
W1	0.117	1.79	0.0654	0.191
W2	0.143	2.03	0.0704	0.186
W3	0.155	0.960	0.161	0.410
C1	0.231	1.53	0.151	0.314
C2	0.447	5.93	0.075	0.113
C3	0.411	0.258	1.59	2.48
C4	0.365	0.433	0.843	1.40
C5	0.478	0.353	1.35	1.96
C6	0.471	0.297	1.59	2.31

[a] Mean value for phenanthrene desorption rate, equal to α/β. [b] Standard deviation of phenanthrene desorption rates, equal to $\alpha^{0.5}/\beta$.

Two-Parameter Gamma Model. Parameters for fitting the gamma model to desorption data for the 15 samples are listed in Table 3. Values for α were 0.145−0.478, β were 24−0.297 days, and average k_d values were 0.007−1.59 day^{-1}, depending on geosorbent type, initial loading level, and aging time. For herbicide desorption from the same Wagner soil, Pedit and Miller (*46*) found $\alpha = 0.11$, $\beta = 1.0$ day, and mean $k_d = 0.11$ day^{-1}, values very close to those reported in Table 3. Figures 4A and 5A show that the gamma model fit phenanthrene desorption data well for Lachine shale and Wagner soil, but Figure 6A reveals that it was not as successful

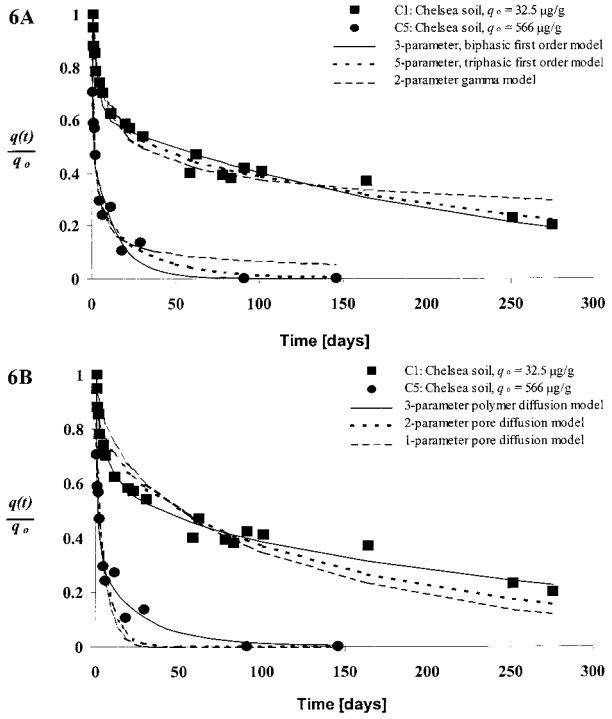

FIGURE 6. Modeling 25 °C phenanthrene desorption from Chelsea soil: (A) multicompartment first-order desorption models and (B) diffusion models.

in fitting the Chelsea soil data. Here the gamma model underpredicted desorption at late times as it "flattened out" too much, indicating that the model does not mechanistically describe the observed desorption process. The calculated α and β parameters do not have obvious physical significance and do not logically correlate to observed trends in slow desorption rates and resistant fractions. There is a strong trend of decreasing values of β with increasing values of the mean k_d, but the β parameter itself does not give any information about the shape of the desorption curve. Mean k_d values logically increase for samples with higher average desorption rates, such as Chelsea soil samples compared to Lachine shale samples. However, from a remediation perspective, the overall average k_d may not be as important as rate constants for slowly desorbing phases. In defense of the gamma model, Figures 4–6 show that it fits desorption data better than the other two-parameter model (the pore-diffusion model with an instantaneously desorbing equilibrium fraction), so it is relatively successful at matching measured data with only two fitting parameters.

Three-Parameter Biphasic Polymer Diffusion Model. The three-parameter, biphasic diffusion model was superior to all other models having three or less parameters, both in terms of visual fits to desorption data and minimal sums of squared residuals. Calculated parameters are listed in Table 4, and model fits to desorption data are given in Figures 4B–6B. Values for D_r/a_r^2 are 0.00031–0.032 day^{-1} and D_s/a_s^2 are 0.000011 to 0.0010 day^{-1}, depending on geosorbent type, phenanthrene loading level, and aging time. Literature values for D_r/a_r^2 are 0.022–0.18 day^{-1} and D_s/a_s^2 are 0.000056–0.000084 day^{-1} for PCB desorption from river sediments (*2*). If effective diffusion distances for rapidly and slowly desorbing fractions were known, then D_r and D_s could be calculated, although diffusion-path lengths are generally much smaller than particle diameters (*2, 3, 7, 30, 31*). A common misconception is that D/a^2 is equivalent to an apparent first-order desorption rate coefficient because its units are reciprocal time. However, a comparison of Tables 4 and 1 reveals that diffusion rate constants are approximately 2 orders of magnitude lower than apparent first-order rate constants for both the rapidly and slowly desorbing fractions. Similar to the first-order biphasic desorption model, however, the ratios of rapid and slow rate parameters, $(D_r/a_r^2)/(D_s/a_s^2)$, ranged from 15 to 136. Although the polymer diffusion model fits desorption data slightly better than the biphasic first-order model, it has a minor disadvantage in that it is computationally more demanding.

One-Parameter Pore-Diffusion Model. The one-parameter pore-diffusion model was inferior to all other models evaluated, both in terms of visual fit to the measured phenanthrene desorption data and the sums of squared residuals. However, this model did fit desorption data better than did a one-parameter first-order desorption model (data not shown). Values for D_{app}/r^2 (often reported as the "effective diffusion coefficient," D_{eff}, when multiplied by the particle radius squared) ranged from 0.000044 to 0.0207 day^{-1}, depending on geosorbent type, initial phenanthrene loading, and aging time. Reported ranges of observed values for D_{eff} of HOC desorption from soils and sediments include 10^{-9}–10^{-12} cm^2/s (*25*), 10^{-17}–10^{-18} cm^2/s (*5*), and 10^{-9}–10^{-10} cm^2/s (*24*). We do not report D_{eff} because effective diffusion length is often not equal to particle radius (*2, 3, 7, 30, 31*). Figures 4B–6B reveal that the pore diffusion model consistently underpredicted desorption at short and intermediate times

TABLE 4. Phenanthrene Desorption Rate Parameters for the Diffusion Rate Models

	two-compartment, three-parameter polymer diffusion model				pore-diffusion, two-parameters	
sample	ϕ_r	$(D_r/a_r^2) \times 10^3$ [days^{-1}]	$(D_s/a_s^2) \times 10^5$ [days^{-1}]	pore-diffusion, one-parameter $(D_{app}/r^2) \times 10^4$ [days^{-1}]	X_1	$(D_{s,app}/r^2) \times 10^4$ [days^{-1}]
L1	0		1.10	0.437	0	0.441
L2	0		1.24	0.490	0	0.494
L3	0.294	0.385	2.58	2.45	0.024	2.29
L4	0.3053	0.311	1.46	1.92	0.024	1.73
L5	0.3371	1.01	2.57	3.64	0.076	2.86
L6	0.342	1.39	2.60	3.90	0.087	2.96
W1	0.249	1.03	0.759	1.74	0.053	1.28
W2	0.229	1.55	1.63	2.21	0.060	1.67
W3	0.258	2.88	2.93	3.29	0.084	2.46
C1	0.282	3.39	6.35	6.02	0.087	4.74
C2	0.114	9.68	19.1	10.2	0.026	9.52
C3	0.6405	4.11	5.86	30.0	0.196	14.1
C4	0.757	4.00	6.23	73.1	0.080	55.8
C5	0.549	17.4	82.1	165	0.058	178
C6	0.468	32.2	99.9	207	0.080	131

and overpredicted desorption at long times. The only data set for which the pore-diffusion model adequately fits the data is sample L1, but all six models fit the data for this sample because it essentially had no rapidly desorbing fraction.

Two-Parameter Pore-Diffusion Model. There have been reports of the pore-diffusion model fitting entire desorption data sets, but desorption rates in those cases were measured over periods of only 2 or so days (*25*). Other studies have shown that the pore-diffusion model does not fit desorption rate data unless it is assumed that a fraction of the sorbed HOC achieves instantaneous equilibrium with the solution phase at the outset of desorption (*22*−*24*, *30*, *31*). To accommodate this assumption, an extra parameter must be added to the model; i.e., X_1, the instantaneous equilibrium fraction. Figures 4B−6B illustrate that the X_1 adjustment improves model fits as compared to the one-parameter version of the pore model but that performance is still poor relative to the other models. Table 4 shows that X_1 values range from 0 to 0.196, depending on geosorbent type, initial phenanthrene loading, and aging time. Model fits still consistently underpredict desorption at intermediate times and overpredict desorption at long times. If the pore diffusion model is expanded to include multiple compartments, each with a characteristic diffusion coefficient, performance improves dramatically (*19*, *22*). For example, by adding a third fitting parameter the pore diffusion model can be converted to a form that is functionally the same as the three-parameter biphasic polymer-diffusion model discussed previously.

Summary of Model Comparisons. The three-parameter biphasic polymer-diffusion model and the three-parameter biphasic first-order desorption model are recommended for simulating rates of phenanthrene desorption from geosorbents. Of these two models, the biphasic polymer-diffusion model gives better fits to experimental data, but the biphasic first-order desorption model is less computationally demanding. A more complex five-parameter triphasic first-order desorption model is not recommended over the biphasic first-order model. The gamma model fit much of the data fairly well, given that it uses only two fitting parameters. That model was not as successful as the three-parameter biphasic desorption and diffusion models at fitting all of the data sets, however, and the physical significances of its parameters are not as readily interpretable. Finally, a spherical pore-diffusion model was not adequate for describing the experimental rate data, even when an instantaneous equilibrium compartment was included. If a pore-diffusion model is used, one with more than two fitting parameters is required.

Selecting a single model to describe desorption rates for all systems assumes that the rate-limiting step is the same in all systems studied. This may not be the case for the systems we studied and describe in this paper, and in general it is almost certainly not the case for all environmental systems. Appropriate choice of a model to describe HOC desorption rates may in fact be a system-specific issue; i.e., one that depends on the nature of the rate-limiting step involved. The two models identified above, the three-parameter biphasic first-order desorption model and the three-parameter biphasic polymer-diffusion model, appear to be particularly good starting points for evaluating various models for desorption of hydrophobic contaminants from natural sorbents.

Acknowledgments

We thank Tom Yavaraski, Julian Garro, and Dr. Hong Fang for invaluable assistance in the experimental phases of this work and Dr. Pierre Goovaerts and Tom Phelan for helpful suggestions regarding numerical methods for modeling the experimental data. Funding for the research was provided in part by the Great Lakes and Mid-Atlantic Center for Hazardous Substance Research, under a grant from the Office of Research and Development, U.S. Environmental Protection Agency. Partial funding of the research activities of this Center was also provided by the State of Michigan Department of Environmental Quality. The content of this publication does not necessarily represent the views of either agency. Partial support was also provided in the form of EPA STAR graduate environmental education fellowship awards to Martin D. Johnson and T. Michael Keinath II.

Literature Cited

(1) Coates, J. T. *J. Contam. Hydrol.* **1986**, *1*, 191−210.
(2) Carroll, K. M.; Harkness, M. R.; Bracco, A. A.; Balcarcel, R. R. *Environ. Sci. Technol.* **1994**, *28*, 253−258.
(3) Pignatello, J. J.; Ferrandino, F. J.; Huang, L. Q. *Environ. Sci. Technol.* **1993**, *27*, 1563−1571.
(4) Scribner, S. L.; Benzing, T. R.; Sun, S. B.; Boyd, S. A. *J. Environ. Qual.* **1992**, *21*, 115−120.
(5) Steinberg, S. M.; Pignatello, J. J.; Sawhney, B. L. *Environ. Sci. Technol.* **1987**, *21*, 1201−1208.
(6) Connaughton, D. F.; Stedinger, J. R.; Lion, L. W.; Shuler, M. L. *Environ. Sci. Technol.* **1993**, *27*, 2397−2403.
(7) Cornelissen, G.; van Zuilen, H.; van Noort, P. C. M. *Chemosphere* **1999**, *38*, 2369−2380.
(8) Ten Hulscher, T. E. M.; Vrind, B. A.; Van den Heuvel, H.; Van der Velde, L. E.; Van Noort, P. C. M.; Beurskens, J. E. M.; Govers, H. A. J. *Environ. Sci. Technol.* **1999**, *33*, 126−132.
(9) McGroddy, S. E.; Farrington, J. W. *Environ. Sci. Technol.* **1995**, *29*, 1542−1550.
(10) Pavlostathis, S. G.; Mathavan, G. N. *Environ. Sci. Technol.* **1992**, *26*, 532−538.
(11) White, J. C.; Hunter, M.; Nam, K. P.; Pignatello, J. J.; Alexander, M. *Environ. Toxicol. Chem.* **1999**, *18*, 1720−1727.
(12) Scow, K. M.; Hutson, J. *Soil Sci. Soc. Am. J.* **1992**, *56*, 119−127.
(13) Nam, K.; Alexander, M. *Environ. Sci. Technol.* **1998**, *32*, 71−74.
(14) Lueking, A. D.; Huang, W. L.; Soderstrom-Schwarz, S.; Kim, M. S.; Weber, W. J., Jr. *J. Environ. Qual.* **2000**, *29*, 317−323.
(15) Allen-King, R. M.; Groenevelt, H.; Warren, C. J.; Mackay, D. M. *J. Contam. Hydrol.* **1996**, *22*, 203−221.
(16) Alexander, M. *Environ. Sci. Technol.* **1995**, *29*, 2713−2717.
(17) Brusseau, M. L. *Environ. Sci. Technol.* **1991**, *25*, 134−142.
(18) Nkedi-Kizza, P.; Brusseau, M. L.; Rao, P. S. C.; Hornsby, A. G. *Environ. Sci. Technol.* **1989**, *23*, 814−820.
(19) Arocha, M. A.; Jackman, A. P.; McCoy, B. J. *Environ. Sci. Technol.* **1996**, *30*, 1500−1507.
(20) Ball, W. P.; Roberts, P. V. *Environ. Sci. Technol.* **1991**, *25*, 1237−1249.
(21) Cornelissen, G.; van Noort, P. C. M.; Govers, H. A. J. *Environ. Sci. Technol.* **1998**, *32*, 3124−3131.
(22) Grathwohl, P.; Reinhard, M. *Environ. Sci. Technol.* **1993**, *27*, 2360−2366.
(23) Harmon, T. C.; Roberts, P. V. *Environ. Prog.* **1994**, *13*, 1−8.
(24) Werth, C. J.; Reinhard, M. *Environ. Sci. Technol.* **1997**, *31*, 697−703.
(25) Wu, S. C.; Gschwend, P. M. *Environ. Sci. Technol.* **1986**, *20*, 717−725.
(26) Veith, W. R. *Diffusion in and Through Polymers: Principles and Applications*; Oxford University Press: New York, 1991.
(27) Rogers, C. E. *The Physics and Chemistry of the Organic Solid State*; Interscience Publishers: New York, 1965; Vol. 2.
(28) Pignatello, J. J.; Xing, B. S. *Environ. Sci. Technol.* **1996**, *30*, 1−11.
(29) Xing, B. S.; Pignatello, J. J. *Environ. Sci. Technol.* **1997**, *31*, 792−799.
(30) Farrell, J.; Reinhard, M. *Environ. Sci. Technol.* **1994**, *28*, 63−72.
(31) Farrell, J.; Grassian, D.; Jones, M. *Environ. Sci. Technol.* **1999**, *33*, 1237−1243.
(32) Ditoro, D. M.; Horzempa, L. M. *Environ. Sci. Technol.* **1982**, *16*, 594−602.
(33) Karickhoff, S. W. In *Contaminats and Sediments*; Baker, R. A., Ed.; Ann Arbor Science: Ann Arbor, 1980; Vol. 2, pp 193−205.
(34) Pignatello, J. J. *Environ. Toxicol. Chem.* **1990**, *9*, 1117−1126.
(35) Cornelissen, G.; van Noort, P. C. M.; Govers, H. A. J. *Environ. Toxicol. Chem.* **1997**, *16*, 1351−1357.
(36) Karickhoff, S. W.; Morris, K. R. *Environ. Toxicol. Chem.* **1985**, *4*, 469−479.
(37) Pignatello, J. J. *Environ. Toxicol. Chem.* **1991**, *10*, 1399−1404.
(38) Pignatello, J. J. *Environ. Toxicol. Chem.* **1990**, *9*, 1107−1115.

(39) Cornelissen, G.; van Noort, P. C. M.; Parsons, J. R.; Govers, H. A. J. *Environ. Sci. Technol.* **1997**, *31*, 454−460.
(40) Kan, A. T.; Fu, G. M.; Tomson, M. B. *Environ. Sci. Technol.* **1994**, *28*, 859−867.
(41) Kan, A. T.; Fu, G.; Hunter, M.; Chen, W.; Ward, C. H.; Tomson, M. B. *Environ. Sci. Technol.* **1998**, *32*, 892−902.
(42) Weber, W. J., Jr.; Huang, W. L.; Yu, H. *J. Contam. Hydrol.* **1998**, *31*, 149−165.
(43) Huang, W. L.; Weber, W. J., Jr. *Environ. Sci. Technol.* **1997**, *31*, 2562−2569.
(44) Huang, W. L.; Weber, W. J., Jr. *Environ. Sci. Technol.* **1998**, *32*, 3549−3555.
(45) Weber, W. J., Jr.; Huang, W. L. *Environ. Sci. Technol.* **1996**, *30*, 3130−3131.
(46) Pedit, J. A.; Miller, C. T. *Environ. Sci. Technol.* **1994**, *28*, 2094−2104.
(47) MacKay, D. M.; Shiu, W. Y. *J. Chem. Eng. Data* **1977**, *22*, 399−402.
(48) Karickhoff, S. W.; Brown, D. S.; Scodd, T. A. *Water Res.* **1979**, *13*, 241−248.
(49) Durand, B. *Kerogen: Insoluble Organic Matter from Sedimentary Rocks*; Techip: Paris, 1980.
(50) Tissot, B. P.; Welte, D. H. *Petroleum Formation and Occurrence*; Springer-Verlag: New York, 1984.
(51) Young, T. M.; Weber, W. J., Jr. *Environ. Sci. Technol.* **1995**, *29*, 92−97.
(52) Johnson, M. D.; Huang, W. L.; Dang, Z.; Weber, W. J., Jr. *Environ. Sci. Technol.* **1999**, *33*, 1657−1663.
(53) Huang, W. L.; Young, T. M.; Schlautman, M. A.; Yu, H.; Weber, W. J., Jr. *Environ. Sci. Technol.* **1997**, *31*, 1703−1710.
(54) Young, T. M.; Weber, W. J., Jr. *Environ. Sci. Technol.* **1997**, *31*, 1692−1696.
(55) Weber, W. J., Jr.; Young, T. M. *Environ. Sci. Technol.* **1997**, *31*, 1686−1691.
(56) Weber, W. J., Jr.; McGinley, P. M.; Katz, L. E. *Environ. Sci. Technol.* **1992**, *26*, 1955−1962.
(57) McGinley, P. M.; Katz, L. E.; Weber, W. J., Jr. *Environ. Sci. Technol.* **1993**, *27*, 1524−1531.
(58) Johnson, M. D.; Weber, W. J., Jr. *Environ. Sci. Technol.* **2001**, *35*, 427−433.
(59) Hawthorne, S. B.; Yang, Y.; Miller, D. J. *Anal. Chem.* **1994**, *66*, 2912−2920.
(60) Deitsch, J. J.; Smith, J. A.; Culver, T. B.; Brown, R. A.; Riddle, S. A. *Environ. Sci. Technol.* **2000**, *34*, 1469−1476.
(61) Berens, A. R.; Huvard, G. S. *J. Dispersion Sci. Technol.* **1981**, *2*, 359−378.
(62) Berens, A. R. *Polymer* **1977**, *18*, 697−704.
(63) Crank, J. *The Mathematics of Diffusion*, 2nd ed.; Oxford Science Publishers: New York, 1975.
(64) Leboeuf, E. J.; Weber, W. J., Jr. *Environ. Sci. Technol.* **1997**, *31*, 1697−1702.
(65) Cornelissen, G.; van der Pal, M.; van Noort, P. C. M.; Govers, H. A. J. *Chemosphere* **1999**, *39*, 1971−1981.

Received for review June 16, 2000. Revised manuscript received January 17, 2001. Accepted January 24, 2001.

ES001391K